Phase Matching Using the Linear Electro-Optic Effect

Zijian Cui,[1,2] Dean Liu,[1,3,*] Jie Miao,[1] Aihua Yang,[1,2] and Jianqiang Zhu[1,3]
[1]Key Laboratory of High Power Laser and Physics, Shanghai Institute of Optics and Fine Mechanics, Chinese Academy of Sciences, Shanghai 201800, China
[2]University of Chinese Academy of Sciences, Beijing 100049, China
[3]Collaborative Innovation Center of IFSA, Shanghai Jiao Tong University, Shanghai 200240, China
(Received 6 August 2016; published 27 January 2017)

Phase matching is a necessary condition for achieving high-efficiency optical-frequency conversion. To date, practical means of accomplishing phase matching in homogeneous crystals remain limited, despite considerable efforts. Herein, we report a new class of methods aimed at achieving quasiperfect phase matching, based on controllable birefringence produced via the linear electro-optic effect, termed "voltage-tuning phase matching." The wave vectors of the induced polarization and the generated fields can be matched and maintained along the direction of propagation by introducing an external electric field. We analyze the validity and feasibility of this method theoretically and demonstrate it experimentally by applying the linear electro-optic effect and fourth-harmonic generation simultaneously in a partially deuterated KH_2PO_4 crystal. Quasiperfect phase matching is achieved systematically over a temperature range of the initial phase-matching temperature ± 2 °C. Moreover, this method can overcome the limitation of the birefringence in traditional technologies and provides new functionalities for conventional nonlinear materials as well as low-birefringence and isotropic materials. This technology may significantly impact the study of optical-frequency conversion and has promise for a broad range of applications in nonlinear optics.

DOI: 10.1103/PhysRevLett.118.043901

Nonlinear optical-frequency conversion has greatly expanded the practical utility of lasers and has exhibited significant scientific and technological potential in many fields. It not only offers a highly efficient way to obtain coherent light at new wavelengths [1–3] but also has become a powerful tool for researchers involved in physics [4–6], chemistry [7,8], and biomedicine [9,10]. For achieving a high conversion efficiency, phase matching between interacting waves is a necessary condition [1,2]. However, owing to the material dispersion, a phase mismatch (Δk) occurs. Precise compensation of dispersion-caused phase mismatch is the primary challenge, which has been addressed in various ways [11–16].

At present, commonly used techniques are birefringent phase matching (BPM), noncritical phase matching (NCPM), and quasiphase matching (QPM) [15–19]. BPM and NCPM exploit the dependences of the refractive index on the wavelength, polarization, and propagation directions of the optical field and on the temperature of the nonlinear material [17–19]. QPM applies a periodic or quasiperiodic structure in the nonlinear material. The sign of the nonlinear susceptibility is reversed periodically by reversing the crystal orientation of the material; the phase mismatch can thus be corrected periodically [11–13]. Overall, these methods aim to suppress phase mismatch in order to facilitate the nonlinear interaction between fields in a favorable direction.

However, despite considerable efforts, there are very few practical methods for achieving quasiperfect phase matching in homogeneous crystals. Angle and temperature tuning (i.e., BPM and NCPM) are the most common methods [16–19] but are very sensitive to the crystal orientation, the temperature, and the laser wavelength [18–21]. Even a small change in these parameters can cause a phase mismatch that is detrimental to frequency conversion and limits the conversion efficiency. Although methods have been proposed to mitigate these undesirable effects [22,23], phase matching remains impossible in principle. The key issue is that the refractive indices associated with the interacting waves are difficult to control precisely.

In this Letter, we propose a novel class of phase-matching methods based on the linear electro-optic effect, termed "voltage-tuning phase matching" (VTPM). In the presence of an external electric field, the refractive index of many nonlinear materials [e.g., β-BaB_2O_4 (BBO), KH_2PO_4, KD_2PO_4 (DKDP), and $LiNbO_3$] depends on the electric-field intensity because of the linear electro-optic effect and can therefore be finely tuned by adjusting the applied voltage [24–26]. The underlying mechanism of the VTPM method involves the application of an external electric field to a nonlinear material, which changes the refractive index and the phase velocity of optical waves. The wave vectors of the interacting optical waves can then be matched and maintained along the direction of propagation during the frequency-conversion process. Quasiperfect phase matching can thus be achieved.

As a representative process, consider the second-harmonic generation (SHG). The evolution of SHG under the condition of phase mismatch is illustrated in Fig. 1(a). With the propagation of waves, the phase lag between the nonlinear polarization and the generated waves gradually accumulates and eventually reaches π, resulting in

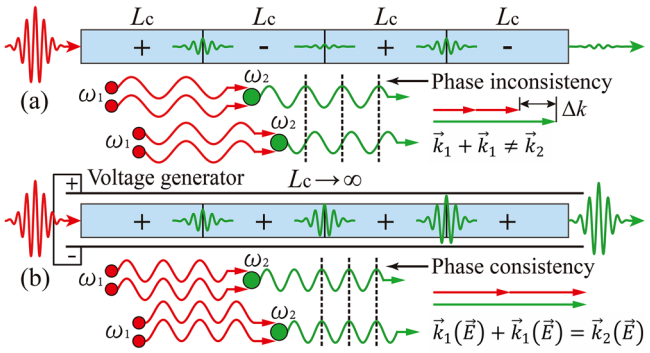

FIG. 1. Schematic of (a) SHG under condition of phase mismatch and (b) SHG with VTPM.

destructive interference and the back-conversion of optical power flows into the fundamental wave. The propagation distance at which destructive interference occurs is defined as the coherence length $L_c = \pi/\Delta k$ [11–13]. The unidirectional frequency conversion is thus restricted to L_c, and a larger Δk yields a smaller L_c. Constructive and destructive interference occur alternately with a period of L_c. Figure 1(b) outlines the wave interpretation of SHG with VTPM. The nonlinear polarization continues to add constructively to the generated waves. Consequently, optical waves generated at each position in the material have the same phase. Their superposition can enhance the total amplitude (constructive interference), yielding the maximum conversion efficiency.

In addition, this idea offers new functionalities and exciting possibilities for many materials. For instance, normal phase matching is impossible to achieve for low-birefringence materials such as $BaTiO_3$ [24]. However, our proposed method can artificially increase the birefringence by controlling the refraction index and can thus achieve quasiperfect phase matching. Furthermore, the traditional phase-matching techniques do not function in isotropic materials because of the lack of birefringence. As a result, the applications of many cubic materials (e.g., ZnTe and GaAs) in nonlinear optics are very limited, even though these materials have attractive nonlinear optical properties [11,14]. If an external electric field is introduced, artificial birefringence can be produced and controlled in these isotropic materials. Regarding the refractive-index ellipsoid, the originally spherical surface is stretched, compressed, or both along specific directions and becomes an ellipsoidal surface. In this way, the limitation of the birefringence for isotropic materials can be overcome. The availability of many materials can thus be increased significantly, and functions that are normally impossible become possible. Taking the materials of space group $\bar{4}3m$ as a typical example, Figs. 2(a) and 2(b) clearly show the variation of the refractive-index ellipsoid with an external electric field along the z axis.

Because the voltage is nonmechanically tunable with a high degree of precision, this method allows quasiperfect phase matching to be achieved systematically and the

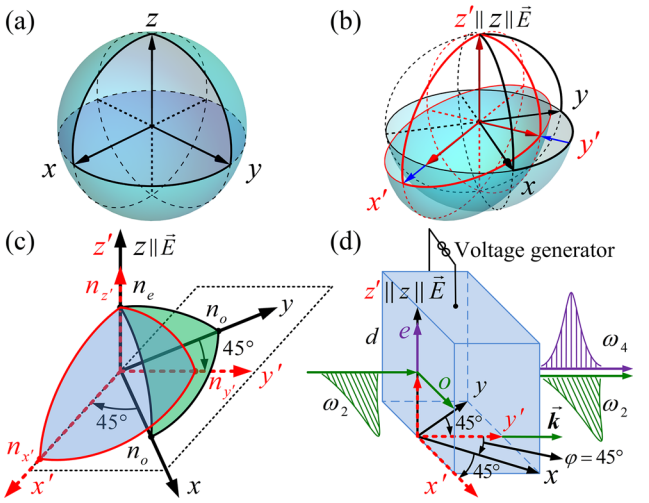

FIG. 2. (a) Refractive-index ellipsoid of a cubic material. Refractive-index ellipsoid variation for (b) a cubic material of space group $\bar{4}3m$ and (c) a DKDP crystal (1/8) with an external electric field along the z axis. (d) Type-I VTPM fourth-harmonic generation (FHG) achieved in a DKDP crystal. The black solid and red dashed arrows indicate the principal axes of the refractive-index ellipsoid in the absence and presence, respectively, of an external electric field.

associated sensitivities to the angle, temperature, and wavelength to be fundamentally overcome. To verify the validity and feasibility of VTPM method convincingly, we designed an ingenious experiment based on the analysis of the linear electro-optic effect and the phase-matching characteristics of a DKDP crystal [17–19].

DKDP is an electro-optic and nonlinear crystal commonly used for its favorable optical properties and high optical uniformity [18,26]. Transverse electro-optic modulation is usually adopted when DKDP is used as an electro-optic crystal. The electric field is directed parallel to the optical axis (z axis), and the optical waves propagate perpendicular to the electric-field direction. In this case, DKDP becomes a biaxial crystal, and the new principal axes x' and y' are rotated by 45° relative to the original x and y axes (standard crystallographic coordinate system) around the z axis, as shown in Fig. 2(c). The relationships between the new and original principal refractive indices are as follows [17]:

$$n_{x'} = n_o - n_o^3 r_{63} E/2, \quad (1)$$

$$n_{y'} = n_o + n_o^3 r_{63} E/2, \quad (2)$$

$$n_{z'} = n_e, \quad (3)$$

where n_o and n_e are the ordinary and extraordinary refractive indices, respectively; $n_{x'}$, $n_{y'}$, and $n_{z'}$ are the new principal refractive indices; r_{63} is the linear electro-optic coefficient; and $E = V/d$ is the electric-field intensity, where V and d are the voltage and crystal height, respectively.

As a nonlinear crystal, DKDP can achieve not only second- and third-harmonic generation by BPM but also the NCPM FHG of 1-μm lasers near room temperature [18,24]. Figure 2(d) shows the type-I NCPM FHG using a

DKDP crystal. It allows the second harmonic (ω_2) with ordinary (o) polarization to enter the crystal and generate a fourth harmonic (ω_4) with extraordinary (e) polarization. The azimuthal angle is generally set as 45° to obtain the most effective nonlinear coefficient [24], as shown by φ in Fig. 2(d). Therefore, the optical waves propagate exactly along the y' axis when an external electric field parallel to the z axis is applied to the DKDP crystal. Furthermore, the respective polarization directions of the interacting waves are unchanged according to the theory of optical-wave propagation in uniaxial and biaxial crystals [27,28]. For a narrow-band laser, according to the slowly varying envelope and plane-wave approximation, the corresponding nonlinear coupled-wave equations can be written as [23,29]

$$\frac{\partial A_2(z)}{\partial z} = \frac{i\omega_2}{n_{2o}c} d_{\text{eff}} A_4(z) A_2^*(z) \exp(i\Delta k \cdot z), \quad (4)$$

$$\frac{\partial A_4(z)}{\partial z} = \frac{i\omega_4}{2n_{4e}c} d_{\text{eff}} A_2(z) A_2(z) \exp(-i\Delta k \cdot z), \quad (5)$$

where the subscripts 2 and 4 represent the second and fourth harmonics, respectively; A and ω are the complex amplitude and angular frequency of the optical field, respectively; c and z represent the velocity of light in vacuum and the propagation distance, respectively; d_{eff} is the effective nonlinear coefficient; and $\Delta k = k_{4e}\text{-}2k_{2o} = 2\omega_2[n_e(\omega_4) - n_o(\omega_2)]/c$ is the phase mismatch, where k represents the wave vector.

For a phase-matching temperature T_0 [$\Delta k(T_0) = 0$], the refractive indices of ω_2 and ω_4 for the DKDP crystal obey $n_o(\omega_2, T_0) = n_e(\omega_4, T_0)$. When the temperature changes to T ($T \neq T_0$), a phase mismatch results from the difference in thermo-optic coefficients between the ordinary and extraordinary waves [24], and the conversion efficiency is hence significantly reduced [18]. If an external electric field is applied along the z axis, the refractive index of ω_2 is related to the electric-field intensity, whereas that of ω_4 is not. The refractive indices of ω_2 and ω_4 and the phase mismatch can be written explicitly as

$$n_{x'}(\omega_2, T, E) = n_o(\omega_2, T) - n_o^3(\omega_2, T) r_{63} E/2, \quad (6)$$

$$n_{z'}(\omega_4, T) = n_e(\omega_4, T), \quad (7)$$

$$\Delta k = 2\omega_2[n_{z'}(\omega_4, T) - n_{x'}(\omega_2, T, E)]/c. \quad (8)$$

An appropriate voltage can be chosen so that the refractive indices of the interacting waves satisfy $n_{x'}(\omega_2, T, E) = n_{z'}(\omega_4, T)$. The phase mismatch induced by temperature variations can be precisely compensated for. The temperature dependence of the voltage is given by

$$V(T) = 2d \frac{n_o(\omega_2, T) - n_e(\omega_4, T)}{n_o^3(\omega_2, T) r_{63}}. \quad (9)$$

Thus, temperature-insensitive FHG can be achieved by applying the linear electro-optic effect to the FHG process. This scheme is particularly suitable for experimentally verifying our proposed method. Moreover, the advantages (e.g., the weak angle sensitivity and the absence of beam walk-off [18]) of NCPM exist in VTPM because optical waves propagate along the principal optical axis (y').

In a DKDP crystal with a different deuterium content, NCPM FHG requires a different phase-matching temperature [18,19]. We chose two DKDP crystals with deuterium contents of 65% and 70% to experimentally verify the proposed method. Our proof-of-principle experiment used a Q-switched Nd:YLF laser (wavelength 1,053 nm) with an 8.5-ns-long (FWHM) Gaussian pulse as the fundamental laser source (ω_1). The transverse profile was approximated by a circle 7 mm in diameter. The output energy was 58.7 mJ per pulse, with a repetition rate of 1 Hz. A 10-mm-thick BBO crystal was used to generate ω_2 (526.5 nm). Two DKDP crystals ($15 \times 15 \times 20$ mm) were cut for type-I NCPM ($\theta_{\text{FHG}} = 90°$ and $\varphi_{\text{FHG}} = 45°$) to generate ω_4 (263.25 nm). A voltage generator (Lasermetrics 5046ER) with a practical operating range of 0–11 kV and a control precision of 0.2 kV was employed.

The generated ω_2 was separated from the residual ω_1 by dichroic mirrors (ω_1 transmission and ω_2 reflection) and was then incident onto the DKDP crystal, which was mounted in a temperature-controlling device that varied the temperature from 1 to 100 °C with a theoretical control precision of ±0.1°C. The generated ω_4 was separated from the residual ω_2 by a prism and measured with an energy meter (Newport 1936-R). We defined the SHG and FHG efficiencies as $\eta_2 = E(\omega_2)/E(\omega_1)$ and $\eta_4 = E(\omega_4)/E(\omega_2)$, respectively, where $E(\omega_1)$, $E(\omega_2)$, and $E(\omega_4)$ are the energy of initial ω_1, generated ω_2 and ω_4, respectively. The measured $E(\omega_2)$ was 12.6 mJ, and the corresponding η_2 was 21.5%.

Temperature-dependent FHG efficiencies were studied for 65%- and 70%-deuterated DKDP crystals, over a temperature range of ±4 °C about the corresponding initial phase-matching temperature. In the experiment, the DKDP crystal temperature was altered over the corresponding range and monitored using an infrared thermal imager (Fluke Ti400). The output fourth-harmonic energy was averaged over 50 measurements at each temperature to eliminate the influence of energy fluctuations. The experimental results are shown in Fig. 3.

Figure 3(a) plots the variation in the FHG efficiencies with temperature for the 65%-deuterated DKDP. The green circles show that the experimental NCPM temperature (T_{NCPM}) was 29.2 °C and the temperature acceptance bandwidth (ΔT_{FWHM}) was 1.24 °C, as defined by the FWHM. The maximum efficiency (η_{max}) was measured to be 6.59% at 29.2 °C. If the DKDP crystal temperature deviated from T_{NCPM}, the phase-matching condition was not satisfied, and the efficiency was dramatically decreased. When the voltage was applied to the DKDP crystal, temperature-insensitive FHG was achieved by adjusting the voltage magnitude. As shown by the magenta squares in Fig. 3(a), ΔT_{FWHM} reached 4.67 °C, which is 3.8 times greater than that for NCPM FHG. Importantly, the measured FHG

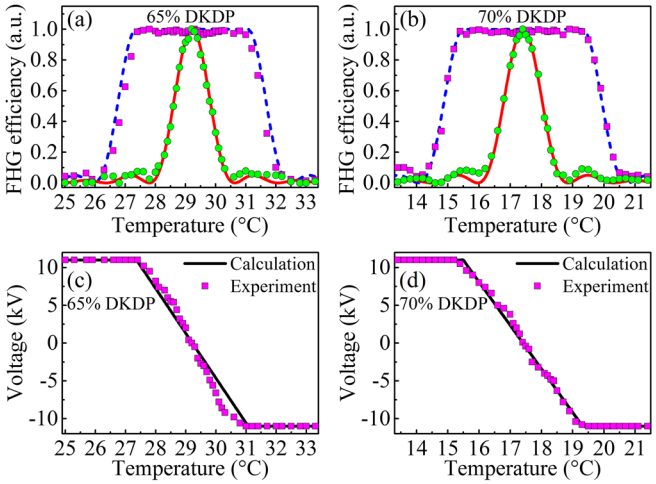

FIG. 3. Experimental and calculated FHG efficiencies obtained using (a) 65%- and (b) 70%-deuterated DKDP, with the corresponding voltages plotted versus temperature in (c) and (d). In (a) and (b), the red solid line and green circles denote the calculated and experimental NCPM FHG efficiencies, respectively; the blue dashed line and magenta squares denote the calculated and experimental VTPM FHG efficiencies, respectively. All the efficiencies are normalized to their maximum values at the corresponding initial phase-matching temperature (29.2 °C and 17.4 °C for the 65%- and 70%-deuterated DKDP crystals, respectively).

efficiencies did not decrease in the range of 27.3–31.1 °C. Their average value and the coefficient of variation were 6.56% and 0.95%, respectively. Thus, quasiperfect phase matching was always achieved in this temperature range, verifying the validity and feasibility of the proposed method.

In the case of 70%-deuterated DKDP, the variation of the experimental NCPM FHG efficiencies with temperature is shown by the green circles in Fig. 3(b). The corresponding T_{NCPM} and ΔT_{FWHM} were 17.4 °C and 1.29 °C, respectively. The measured $\eta_{\max}$ was 6.92%. For VTPM FHG, ΔT_{FWHM} increased to 5.1 °C, which is four times greater than that for NCPM FHG. In the range of 15.4–19.4 °C, the average value and the coefficient of variation of the measured FHG efficiencies were 6.93% and 0.92%, respectively. The phase-matching temperature range was 15.4–19.4 °C, as shown by the magenta squares in Fig. 3(b).

For conventional methods, phase matching was satisfied only at a specific temperature [18–20]. In our experiment, the phase-matching condition was notably always satisfied, and the conversion efficiency was not decreased in the range of $T_{\mathrm{NCPM}} \pm 2$ °C. The applied voltages are plotted as functions of temperature in Figs. 3(c) and 3(d). A larger temperature deviation caused a higher required compensation voltage (V_c). The maximum output voltage ($V_{\max}$) for our voltage generator was 11 kV. When V_c exceeded $V_{\max}$, phase matching could not be achieved, resulting in a decrease in the conversion efficiency, as shown by the magenta squares in Fig. 3. If a voltage generator capable of providing a higher voltage was used, ΔT_{FWHM} and the phase-matching temperature range (PMTR) could be increased further.

TABLE I. Experimental and calculated results of FHG.

		NCPM FHG		VTPM FHG	
DKDP	Parameters	Experiment	Calculate	Experiment	Calculate
65%	$\eta_{\max}$	6.59%	7.04%	6.56%	7.04%
	ΔT_{FWHM}	1.24 °C	1.26 °C	4.67 °C	4.96 °C
	PMTR	···	···	27.3–31.1 °C	27.2–31.3 °C
70%	$\eta_{\max}$	6.92%	7.04%	6.93%	7.04%
	ΔT_{FWHM}	1.29 °C	1.28 °C	5.10 °C	5.11 °C
	PMTR	···	···	15.4–19.4 °C	15.3–19.5 °C

According to Eqs. (4)–(9), the numerically calculated results corresponding to the experimental conditions were plotted together with the experimental results to allow a direct comparison, as shown in Fig. 3. The experimental and calculated results are compared in Table I.

The above comparison shows good agreement between the experimental and calculated data, despite a few discrepancies. These may have been due to imprecise temperature control and fluctuations in the crystal temperature. Nonetheless, the results prove that VTPM method effectively achieved quasiperfect phase matching.

More generally, phase mismatch arising from other causes (e.g., angle variation or wavelength shift) can also be effectively compensated, as the VTPM method displays a high degree of tunability. Our prototype for temperature-insensitive FHG can be adapted accordingly. We consider a 70%-deuterated DKDP crystal as an example to numerically analyze the angle and wavelength sensitivities. The parameters used reflect the experimental conditions. For simplicity, we assume that the SHG output efficiency remains stable and the BBO and DKDP crystals remain at the initial phase-matching temperature. The calculated SHG efficiency is 22.9%, and the FHG efficiencies are plotted in Fig. 4.

Figure 4(a) shows that the angle acceptance bandwidth (ΔA_{FWHM}) for NCPM FHG is 22.43 mrad. In the case of VTPM FHG, ΔA_{FWHM} is 44.81 mrad, which is 2.0 times greater than that for NCPM FHG. Figure 4(b) plots the wavelength-dependent FHG efficiencies. The wavelength acceptance bandwidth (ΔW_{FWHM}) of NCPM FHG is 0.135 nm. For VTPM FHG, ΔW_{FWHM} becomes 4.0 times greater than that for NCPM FHG, increasing to 0.535 nm. In the above calculation, the maximum voltage was assumed to be 11 kV. A voltage generator capable of providing a higher voltage would further increase ΔA_{FWHM}, ΔW_{FWHM}, and the phase-matching range.

Compared with conventional methods, the VTPM method exhibits many significant advantages. First, the angle, temperature, and wavelength phase-matching bandwidths were significantly increased, and quasiperfect phase matching was always satisfied over a wide range. Second, in our experiment, the control precisions of the temperature and voltage reached ±0.1 °C and 0.2 kV, respectively. For the DKDP crystal, $dn_o(T)/dT \approx -3 \times 10^{-5}/°\mathrm{C}$, $dn_e(T)/dT \approx -2 \times 10^{-5}/°\mathrm{C}$, and $|dn_{x'}(V)/dV| = |dn_{y'}(V)/dV| \approx 1.5 \times 10^{-9}/V$ [24]. If the voltage control maps onto the temperature control, the temperature

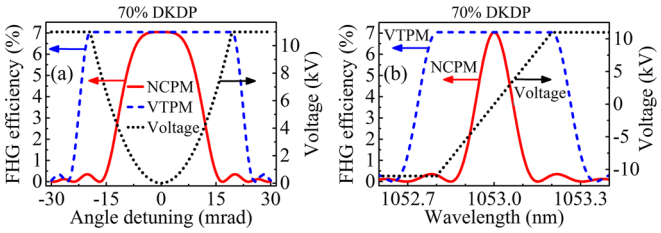

FIG. 4. Calculated NCPM and VTPM FHG efficiencies versus (a) angle and (b) wavelength, for a 70%-deuterated DKDP crystal.

precision can reach ±0.01 °C, which is higher than the control precision of the temperature-controlling device. Third, the response time of voltage tuning is substantially faster than that of temperature tuning.

For many frequency-conversion processes, including the SHG, FHG, sum- and difference-frequency generation and optical parametric amplification, their phase-matching mechanisms are very similar [17–19]. Therefore, the proposed method demonstrated by FHG can be extended to other frequency-conversion processes. Because phase matching plays an important role in many applications and numerous materials exhibit the linear electro-optic effect [24–26], the idea presented here promotes the development of nonlinear optical devices with increased functionality, such as more robust frequency converters and tunable laser sources with improved coherence and stability [30]. In addition, this method can be flexibly combined with other technologies and extended to different fields, including all-optical signal processing, infrared detection, and imaging [31,32]. The aforementioned advantages give this method great practical significance and potential for a broad range of applications.

In summary, we proposed and demonstrated a new phase-matching method based on the linear electro-optic effect. It can achieve quasiperfect phase matching and has numerous remarkable advantages. Temperature-insensitive FHG was demonstrated experimentally. Angle- and wavelength-dependent FHG were analyzed numerically. A basic theoretical framework for applying nonlinear materials using the proposed method was established. The experimental and analytical results support the feasibility and superiority of the method. Thus, this method paves the way for the design of novel nonlinear optical devices and provides a new perspective for the further study of nonlinear optical interactions. Moreover, this idea can endow materials with normally nonexistent characteristics, which may open an avenue for expanding the applications of conventional nonlinear materials and even low-birefringence and isotropic materials. We anticipate that this method will have far-reaching implications in the field of nonlinear optics.

This work is supported by the National Natural Science Foundation of China (Grants No. 11204327 and No. 11304332).

*liudean@siom.ac.cn

[1] J. A. Armstrong, N. Bloembergen, J. Ducuing, and P. S. Pershan, Phys. Rev. **127**, 1918 (1962).
[2] P. A. Franken and J. F. Ward, Rev. Mod. Phys. **35**, 23 (1963).
[3] C. Canalias and V. Pasiskevicius, Nat. Photonics **1**, 459 (2007).
[4] A. M. Pugachev, V. I. Kovalevskii, N. V. Surovtsev, S. Kojima, S. A. Prosandeev, I. P. Raevski, and S. I. Raevskaya, Phys. Rev. Lett. **108**, 247601 (2012).
[5] S. G. Rodrigo, H. Harutyunyan, and L. Novotny, Phys. Rev. Lett. **110**, 177405 (2013).
[6] C. Danson, D. Hillier, N. Hopps, and D. Neely, High Power Laser Sci. Eng. **3**, e3 (2015).
[7] Y. R. Shen, Nature (London) **337**, 519 (1989).
[8] G. L. Richmond, Chem. Rev. **102**, 2693 (2002).
[9] P. J. Campagnola, A. C. Millard, M. Terasaki, P. E. Hoppe, C. J. Malone, and W. A. Mohler, Biophys. J. **82**, 493 (2002).
[10] P. J. Campagnola and L. M. Loew, Nat. Biotechnol. **21**, 1356 (2003).
[11] A. Fiore, V. Berger, E. Rosencher, P. Bravetti, and J. Nagle, Nature (London) **391**, 463 (1998).
[12] A. Paul, R. A. Bartels, R. Tobey, I. Christov, H. Kapteyn, M. Murnane, and S. Backus, Nature (London) **421**, 51 (2003).
[13] A. Bahabad, M. M. Murnane, and H. C. Kapteyn, Nat. Photonics **4**, 571 (2010).
[14] M. Baudrier-Raybaut, R. Haidar, P. Kupecek, P. Lemasson, and E. Rosencher, Nature (London) **432**, 374 (2004).
[15] C. Zhang, Y.-q. Qin, and Y.-y. Zhu, Opt. Lett. **33**, 720 (2008).
[16] A. Rose and D. R. Smith, Opt. Mater. Express **1**, 1232 (2011).
[17] R. W. Boyd, *Nonlinear Optics*, 3rd ed. (Academic Press, New York, 2008).
[18] S. T. Yang, M. A. Henesian, T. L. Weiland, J. L. Vickers, R. L. Luthi, J. P. Bielecki, and P. J. Wegner, Opt. Lett. **36**, 1824 (2011).
[19] L. S. Zhang, F. Zhang, M. X. Xu, Z. P. Wang, and X. Sun, Opt. Express **23**, 23401 (2015).
[20] M. Webb, IEEE J. Quantum Electron. **30**, 1934 (1994).
[21] L. E. Myers, W. R. Bosenberg, R. C. Eckardt, M. M. Fejer, and R. L. Byer, Opt. Lett. **21**, 591 (1996).
[22] Y. K. Yap, K. Deki, N. Kitatochi, Y. Mori, and T. Sasaki, Opt. Lett. **23**, 1016 (1998).
[23] H. Z. Zhong, P. Yuan, S. C. Wen, and L. J. Qian, Opt. Express **22**, 4267 (2014).
[24] D. N. Nikogosyan, *Nonlinear Optical Crystals: A Complete Survey* (Springer, New York, 2005).
[25] A. Yariv and P. Yeh, *Photonics* (Oxford University Press, Oxford, England, 2007).
[26] D. Eimerl, Ferroelectrics **72**, 95 (1987).
[27] J. Yao, W. Sheng, and W. Shi, J. Opt. Soc. Am. B **9**, 891 (1992).
[28] D. A. Roberts, IEEE J. Quantum Electron. **28**, 2057 (1992).
[29] D. Eimerl, J. M. Auerbach, and W. Milonni, J. Mod. Opt. **42**, 1037 (1995).
[30] J. A. Giordmaine and R. C. Miller, Phys. Rev. Lett. **14**, 973 (1965).
[31] A. Ganany-Padowicz, I. Juwiler, O. Gayer, A. Bahabad, and A. Arie, Appl. Phys. Lett. **94**, 091108 (2009).
[32] J. S. Dam, P. Tidemand-Lichtenberg, and C. Pedersen, Nat. Photonics **6**, 788 (2012).